Arabian Journal of Chemistry (2015) xxx, xxx–xxx

King Saud University

Arabian Journal of Chemistry

www.ksu.edu.sa
www.sciencedirect.com

ORIGINAL ARTICLE

Direct chemiluminescence of fluorescent gold nanoclusters with classic oxidants for hydrogen peroxide sensing

Xiaoying You, Yinhuan Li *

School of Science, Xi'an Jiaotong University, Xi'an 710049, China

Received 26 January 2015; accepted 23 May 2015

KEYWORDS

Chemiluminescence;
Gold nanoclusters;
Acidic permanganate;
Hydrogen peroxide

Abstract Direct chemiluminescence (CL) of fluorescent gold nanoclusters was observed for the first time upon oxidation with classic oxidants. The CL mechanism was investigated by the studies of CL spectrum, UV–vis absorption spectra and X-ray photoelectron spectra before and after the reaction. The excited state $Mn(II)^*$, originating from the reduction of permanganate with gold nanoclusters, was suggested as the possible luminophor for the reaction. The potential analytical application was demonstrated by using hydrogen peroxide as an example, based upon the fact that hydrogen peroxide decreased the CL signal significantly. The decreased CL intensity was proportional to the concentration of hydrogen peroxide in the range 1.0×10^{-6}–1.0×10^{-4} mol L^{-1}. The detection limit was 5×10^{-7} mol L^{-1} and the relative standard deviation was 1.4% for 1.0×10^{-5} mol L^{-1} hydrogen peroxide in 11 replicated measurements. This method was applied to the determination of hydrogen peroxide in water samples with satisfactory results.

1. Introduction

Metal nanoclusters (NCs), also known as metal quantum dots, are a fascinating class of nanomaterials that recently attract continuous research interest (Zhang and Wang, 2014; Luo et al. 2014). They are composed of several to hundreds of atoms and have the sizes ranging from subnanometer to approximately 2 nm, bridging the gap between isolated atom and larger nanoparticles. The sizes comparable to Fermi wavelength of the electron make them exhibit molecule-like property and produce size-dependent fluorescence (Zhu et al., 2008). Among the reported metal NCs, Au NCs are the most extensively studied for their attractive features, such as easy synthesis, low toxicity, excellent photo-stability, good biocompatibility, and easy surface functionalization (Chen et al., 2015). The Au NCs have been extensively explored in sensing, enzyme activity assay, protein discrimination, as well as in bioimaging (Chen et al., 2015; Xiong et al., 2015; Sun et al., 2014; Xu et al., 2014; Yu et al., 2014).

Chemiluminescence (CL), light emission produced in a chemical reaction, is an important and powerful technique

* Corresponding author. Tel.: +86 029 82668559; fax: +86 029 82663914.
E-mail address: liyh@mail.xjtu.edu.cn (Y. Li).
Peer review under responsibility of King Saud University.

ELSEVIER Production and hosting by Elsevier

http://dx.doi.org/10.1016/j.arabjc.2015.05.019

for its unique advantages of simplicity, rapidity, and sensitivity (Ocana-Gonzalez et al., 2014; Iranifam, 2014; Waseem et al., 2013; Liu et al., 2010). The exploration of new CL reaction is of paramount importance and highly desirable. To date, reports on the CL reaction involving in metal NCs are relatively rare. Yu and co-workers reported that Ag NCs could strongly enhance the weak CL from the reaction between Ce(IV) and sulphite; copper ions (Yu and Wang, 2011) and cysteine(Yu et al., 2012) were determined based upon their inhibitory effect on the reaction. Deng et al. utilized peroxidase-like catalytic activity of Au NCs to amplify CL signal of luminol-hydrogen peroxide reaction (Deng et al., 2014).

We herein, for the first time, investigated direct CL reaction between bovine serum albumin (BSA)-stabilized Au NCs and five classic oxidants, namely potassium permanganate ($KMnO_4$), cerium(IV) (Ce(IV)), potassium ferricyanide ($K_3Fe(CN)_6$), hydrogen peroxide (H_2O_2), and N-bromosuccinimide (NBS). The experimental variables were optimized and the possible CL mechanism was proposed. The preliminary application of this CL reaction was demonstrated by using H_2O_2 as a model analyte, suggesting that metal NCs-based direct CL reaction can be a promising candidate for the analytical application.

2. Experimental

2.1. Apparatus

CL measurements and data acquisition were carried out on a model IFFM-D flow injection CL analyser (Xi'an Remex Analytic Instrument Co. Ltd., China), which was equipped with a CR105 photomultiplier tube (Hamamatsu Photonics Co. Ltd., China). CL spectrum was obtained by means of a series of interference filters (Institute Biophysics of Chinese Academy of Science, China), which was set between the reaction cell and the window of the photomultiplier tube. UV–vis absorption spectra were scanned on a UV-1800 spectrophotometer (Shimadzu, Japan) with a slit width of 2 nm by using 1 cm cuvette. Fluorescence spectrum was taken on an F-2700 fluorescence spectrophotometer (Hitachi, Japan). Transmission electron microscopy (TEM) image was measured on a JEM-2100 transmission electron microscope (Japan Electronic Company, Japan) at an accelerating voltage of 200 kV. The X-ray photoelectron spectrum (XPS) was measured on an X-ray photoelectron spectrometer (Ultra DLD, Kratos, Britain) using Al-Kα as the exciting source (1486.6 eV) and binding energy calibration was based on C 1s at 284.8 eV.

2.2. Chemicals

All chemicals were of analytical grade; the water was obtained from an AXLC1805 ultrapure water purification system (Beijing ASTK Technology Development Co., Ltd). Chloroauric acid was purchased from Shanghai Chemical Reagent Company, China. Bovine serum albumin (BSA) was purchased from Beijing Xinjingke Biotechnology Company, China. Ammonium cerium (IV) nitrate and N-bromosuccinimide were obtained from Tianjin Fuchen Chemical Reagents Factory, China. Potassium permanganate, potassium ferricyanide, hydrogen peroxide (30%), and other reagents were purchased from Xi'an Chemical Reagent Company, China.

2.3. Synthesis of BSA-stabilized Au NCs

All glassware was cleaned with aqua regia and then rinsed with ultrapure water. BSA-stabilized Au NCs were prepared according to the literature with minor modification (Xie et al. 2009). Briefly, $HAuCl_4$ solution (1.0×10^{-3} mol L^{-1}, 10 mL, 37 °C) was mixed with BSA solution (5.0×10^{-2} g mL^{-1}, 10 mL, 37 °C). After stirring for 2 min, NaOH solution (1.0 mol L^{-1}, 1.0 mL) was added into the mixture. The reaction was allowed to perform at 37 °C for 12 h under stirring. During this period, the colour of the solution gradually changed from light yellow to deep brown.

2.4. Batch CL measurement

Into CL reaction cell, 0.5 mL of oxidant solution and 0.5 mL of reaction medium were added. Then 0.5 mL of the as-prepared Au NCs solution in the dilution of 1:20 was injected to initiate the CL reaction. The CL signal was detected with the photomultiplier tube biasing at high voltage of 600 V.

2.5. Flow injection CL measurements

Fig. 1 shows the schematic diagram of CL flow system. The Au NCs solution (50 μL) was injected into carrier H_2O via syringe, which was then combined with the emerged stream of $KMnO_4$ and diluted H_2SO_4. The CL signal produced in the flow cell was detected by the photomultiplier tube biasing at high voltage of 800 V.

For the detection of H_2O_2, the carrier was replaced with a series of H_2O_2 standards with the concentration range from 1.0×10^{-6} to 1.0×10^{-4} mol L^{-1}. The CL intensity in the absence of H_2O_2 was recorded as I_0 and in the presence of H_2O_2 as I. The decreased CL intensity (ΔI) was calculated by subtracting I from I_0. The calibration curve for H_2O_2 was constructed by plotting ΔI to the concentration of H_2O_2.

3. Results and discussion

3.1. CL of BSA-stabilized Au NCs with classic oxidants

The BSA-stabilized Au NCs were prepared following the previous work of Xie et al. (2009). The as-prepared Au NCs exhibit a red emission peak at 610 nm upon excitation at 490 nm (Fig. S1). The size of Au NCs is less than 2 nm proved by TEM image (Fig. S2). When Au NCs solution was injected

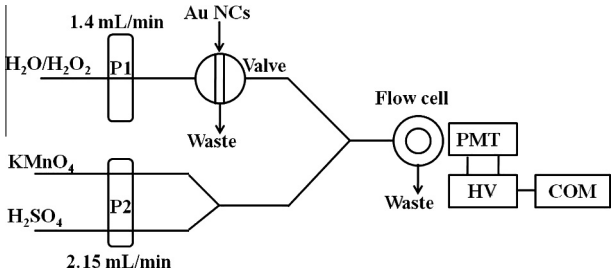

Figure 1 Schematic diagram of CL flow system. P1, P2: peristaltic pump; PMT: photomultiplier tube; HV: high voltage; COM: computer.

into mixed solution of oxidant with reaction medium, strong CL signal was recorded (Fig. 2A). The CL intensities were in the orders of $KMnO_4$ > NBS > $K_3Fe(CN)_6$ > H_2O_2 > Ce(IV). Acidic $KMnO_4$–Au NCs CL reaction was selected to further investigate for its producing highest CL signal. The acidic $KMnO_4$–Au NCs CL reaction is a fast process; the CL intensity reached a maximum after ~1.25 s upon injection of Au NCs. To rule out the possible CL from the reaction between acidic $KMnO_4$ and the reactants used for preparation of Au NCs, control experiments were conducted. As shown in Fig. 2B, no measureable CL signal was recorded for the reaction of acidic $KMnO_4$ with Au(III). And for the reaction between acidic $KMnO_4$ and BSA, only a very weak CL was observed which was much lower than that of acidic $KMnO_4$ with Au NCs. Accordingly, the CL emission was attributed to the reaction between acidic $KMnO_4$ and Au NCs not from other concomitants.

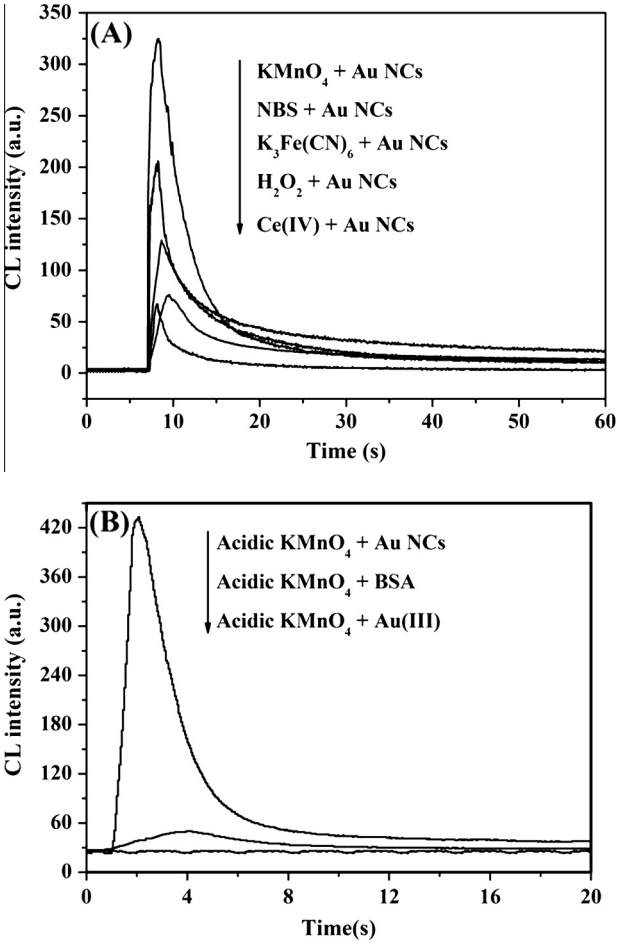

Figure 2 (A) CL profiles of Au NCs with different oxidants. 1:20 Au NCs. The reaction conditions are 5.0×10^{-4} mol L^{-1} $KMnO_4$ in 0.05 mol L^{-1} H_2SO_4, 1.0×10^{-3} mol L^{-1} Ce(IV) in 0.1 mol L^{-1} H_2SO_4, 0.1 mol L^{-1} H_2O_2 in 0.1 mol L^{-1} NaOH, 0.01 mol L^{-1} NBS in 0.5 mol L^{-1} NaOH, and 0.01 mol L^{-1} $K_3Fe(CN)_6$ in 0.5 mol L^{-1} NaOH. (B) CL of acidic $KMnO_4$ with Au NCs, BSA, and Au(III), respectively. 1:20 Au NCs. 2.2×10^{-4} mol L^{-1} Au(III) and 1.09×10^{-3} g mL^{-1} BSA which were the same amounts to Au NCs in the dilution of 1:20.

3.2. CL mechanism of BSA-stabilized Au NCs with acidic $KMnO_4$ reaction

The identification of luminophor is of significant importance for a new CL reaction. The CL spectrum of the reaction was acquired by using a series of filters. The CL reaction had one emission band locating at around 640 nm (Fig. 3). Obviously, Au NCs were not the luminophor of the reaction since the CL spectrum of acidic $KMnO_4$–Au NCs reaction was remarkably different with the fluorescence spectrum of Au NCs. Barnett et al. (2002) and Hindson et al. (2010) have thoroughly investigated the mechanism of acidic permanganate CL system and suggested the excited state $Mn(II)^*$ as the possible luminophor which emits emission around 610–660 nm, assigning to the phosphorescence of Mn(II) (from 4T1 to 6A1 transition). The CL spectrum of this reaction matched well with that of the excited state $Mn(II)^*$. Thus, the excited state $Mn(II)^*$ was suggested as the potential luminophor for this system.

When the Au NCs solution was mixed with acidic $KMnO_4$ solution, the characteristic absorption band of $KMnO_4$ around 530 nm disappeared (Fig. 4), implying that $KMnO_4$ was reduced by Au NCs during reaction. Meanwhile, the purple of $KMnO_4$ solution faded and the colour of the mixture turned into light yellow matching well with the colour of Au(III) solution. Thus, it was deduced that during the reaction Au NCs were oxidized to Au(III), while Mn(VII) was readily reduced to Mn(II) in acid medium. To further identify the oxidation state of gold and manganese after the reaction, XPS experiments were performed. Prior to XPS measurement, the mixture of Au NCs with $KMnO_4$ in 4.0 mol L^{-1} HNO_3 (v/v = 3:1), $KMnO_4$, $MnSO_4$ powder was treated via vacuum-drying for 2 h and the Au NCs were treated by freeze-drying for two days (Zhang et al. 2006). Fig. 5A showed that the Au 4f7/2 band taken from Au NCs located at 84.5 eV, confirming the presence of Au(0) core in Au NCs (Jiang et al. 2014). After the reaction, the Au 4f7/2 band emerged at higher core binding energy (86.3 eV) in the range of Au(III) species (Odio et al. 2014), confirming the formation

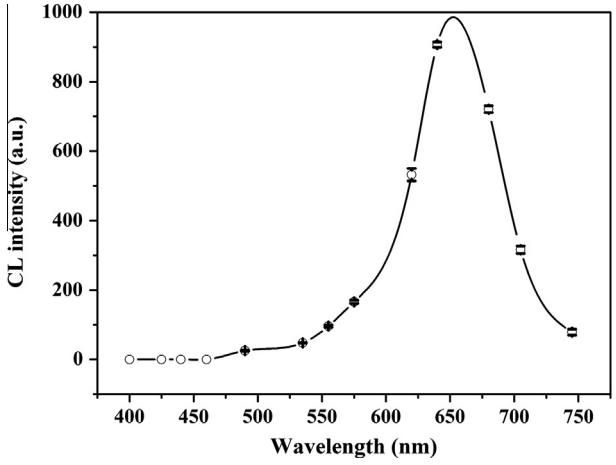

Figure 3 The CL spectrum for the reaction of Au NCs with acidic $KMnO_4$. 5.0×10^{-4} mol L^{-1} $KMnO_4$ in 0.05 mol L^{-1} H_2SO_4, 1:20 Au NCs. The error bars represent standard deviations of three replicate measurements.

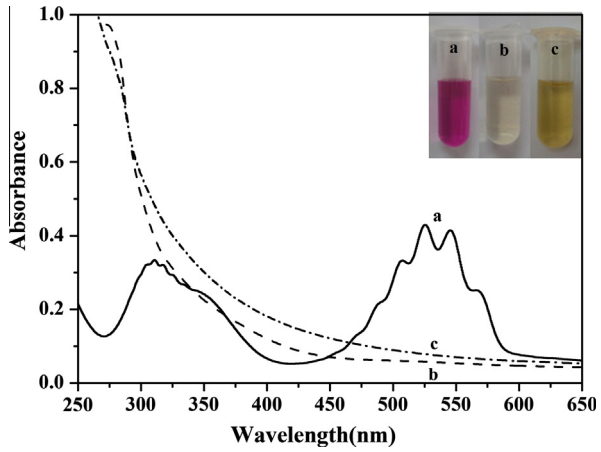

Figure 4 UV–Vis spectra before and after the reaction. (a) 1.0×10^{-4} mol L^{-1} $KMnO_4$ in 0.01 mol L^{-1} H_2SO_4, (b) 1:50 Au NCs, and (c) the mixture of a and b. The inset is the photographs of acidic $KMnO_4$, Au NCs and the mixture.

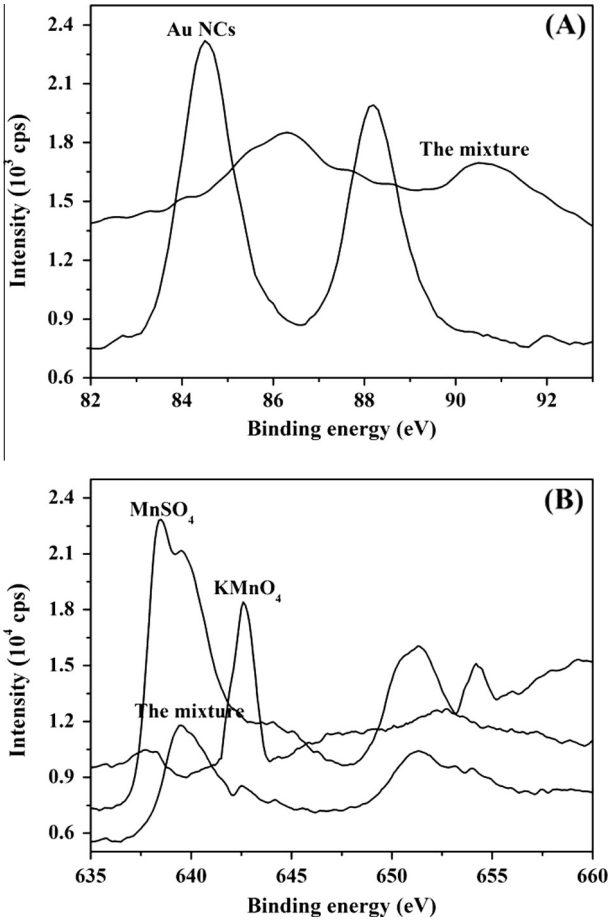

Figure 5 XPS for the (A) Au4f binding energy before and after the CL reaction and (B) Mn2p binding energy in $KMnO_4$, $MnSO_4$ and the mixture.

of Au(III) after the reaction. And for the mixture of $KMnO_4$ with Au NCs, the peak of Mn2p binding energy assigned to Mn(VII) species (642.6 eV) was absent (Fig. 5B), while the band of Mn2p binding energy taken from the mixture of $KMnO_4$ with Au NCs was in good agreement with that of $MnSO_4$ standard, indicating that Mn(VII) species was reduced to Mn(II) after the reaction.

Based on the discussion above, the CL mechanism of the reaction may be attributed, therefore, to the following reactions. $KMnO_4$ was rapidly reduced by Au NCs in an acid medium to produce the excited state $Mn(II)^*$, which returns to the ground state accompanying with CL emission around 640 nm, as illustrated in Scheme 1.

3.3. Effect of experimental variables

To achieve the maximum CL response, the effect of experimental variables, including Au NCs concentration, $KMnO_4$ concentration, and H_2SO_4 concentration was investigated. The CL intensity was strongly dependent on the concentration of the Au NCs employed (Fig. S3A). The higher the Au NCs concentrations the higher the CL signals. The CL intensity increased with $KMnO_4$ concentration up to 5.0×10^{-4} mol L^{-1} and then decreased with further increase in $KMnO_4$ concentration (Fig. S3B). This observation was reported in many acidic $KMnO_4$-based CL system. Most $KMnO_4$ CL systems occur in acidic media and H_2SO_4 is a popular one. The effect of H_2SO_4 concentration was examined in the range 1.0×10^{-3}–0.15 mol L^{-1} (Fig. S3C). The CL intensity had a maximum at 0.05 mol L^{-1} H_2SO_4. Higher or lower concentration of H_2SO_4 caused a decrease in the CL intensity.

3.4. Response of the system to hydrogen peroxide

The detection of hydrogen peroxide (H_2O_2) attracts a great deal of attention due to its involvement in many chemical, biological, and environmental processes. Particularly, H_2O_2 is one of the products of enzymatic reactions, thus enabling quantitative assays of enzyme substrates as well as enzyme activity. We here found that the CL signal of acidic $KMnO_4$–Au NCs system was significantly decreased in the presence of H_2O_2 (Fig. 6A). A linear relationship between the decreased CL intensity and H_2O_2 concentration was achieved in the range of 1.0×10^{-6}–1.0×10^{-4} mol L^{-1} (Fig. 6B). The detection limit, three times standard deviation of blank, was calculated to be 5×10^{-7} mol L^{-1}. The method exhibited good precision with

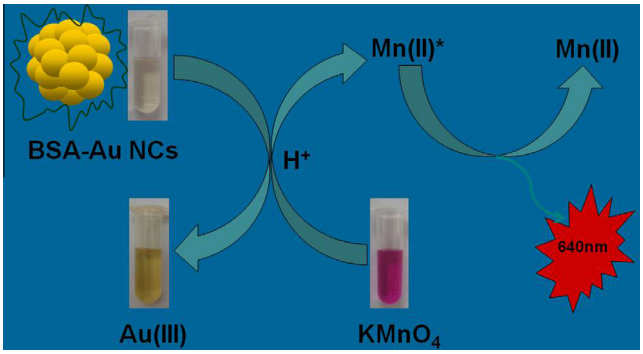

Scheme 1 Schematic illustration of CL mechanism for acidic $KMnO_4$–Au NCs reaction.

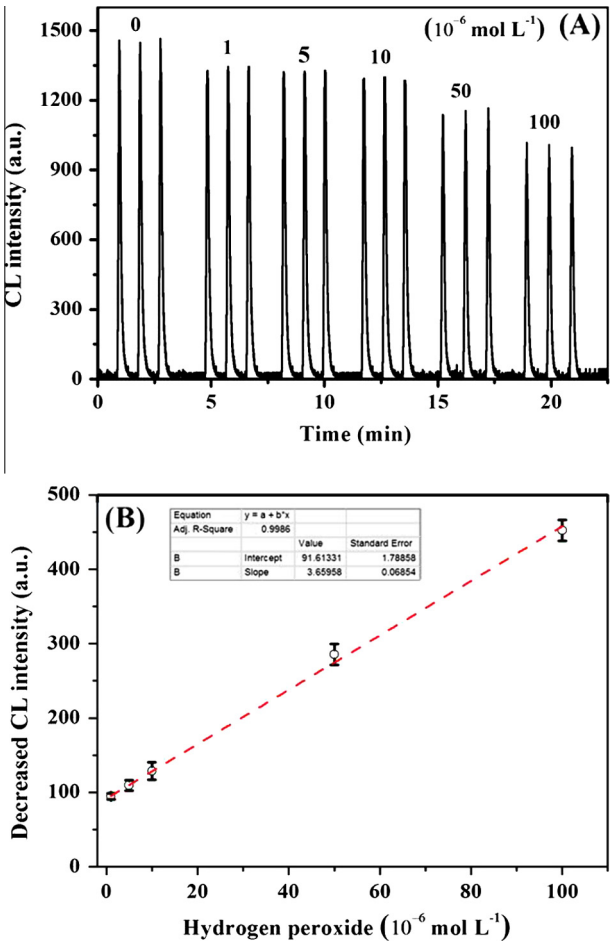

Figure 6 (A) Response to different concentration of H_2O_2 and (B) the linear relationship between the decreased CL intensity and the concentration of H_2O_2. 5.0×10^{-4} mol L^{-1} $KMnO_4$, 0.05 mol L^{-1} H_2SO_4, and 1:20 Au NCs were employed. The error bars represent standard deviations of three replicate measurements.

Table 1 Determination of H_2O_2 in water samples (10^{-6} mol L^{-1}).

Water samples	Added	Found	RSD (n = 3)	Recovery
Rainwater		1.37	2.4%	
	4.00	5.10	2.8%	93.3%
	10.0	11.57	2.3%	102.0%
Drinking mineral water		Not found		
	3.00	2.84	2.0%	94.7%
	6.00	5.57	2.0%	92.8%
	9.00	8.21	2.3%	91.2%
Drinking purified water		Not found		
	3.00	2.92	1.6%	97.3%
	6.00	5.76	2.2%	96.0%
	9.00	8.49	2.8%	94.3%

a relative standard deviation of 1.4% for 1.0×10^{-5} mol L^{-1} hydrogen peroxide in 11 replicated measurements.

To evaluate the potential application of this method for real sample analysis, it was applied to the determination of H_2O_2 in water samples. Rainwater sample was collected from the city of Xi'an and drinking water samples were purchased from the local market. The water samples were filtered using a membrane filter (pore size: 0.45 μm) before analysis. The results are shown in Table 1. The recovery studies were carried out at the same time by adding H_2O_2 standard to water samples. As can be seen from Table 1, the recoveries of added H_2O_2 can be quantitative, demonstrating the method can be used to determine H_2O_2 in water samples.

4. Conclusion

Direct CL reaction between fluorescent Au NCs and classic oxidants was explored. The CL mechanism of acidic $KMnO_4$–Au NCs reaction was thoroughly investigated. The excited state $Mn(II)^*$ was suggested as the potential luminophor. The potential application in the determination of H_2O_2 was demonstrated. This investigation opens new sight into the optical characteristics of the Au NCs. Taking the advantages of metal NCs, it is expected that this work will stimulate more exciting investigation on the CL of metal NCs.

Acknowledgement

The authors gratefully acknowledge financial support from Fundamental Research Funds for the Central Universities.

Appendix A. Supplementary material

Supplementary data associated with this article can be found, in the online version, at http://dx.doi.org/10.1016/j.arabjc.2015.05.019.

References

Barnett, N.W., Hindson, B.J., Jones, P., Smith, T.A., 2002. Chemically induced phosphorescence from manganese(II) during the oxidation of various compounds by manganese(III), (IV) break and (VII) in acidic aqueous solutions. Anal. Chim. Acta 451, 181–188.

Chen, L.Y., Wang, C.W., Yuan, Z.Q., Chang, H.T., 2015. Fluorescent gold nanoclusters: recent advances in sensing and imaging. Anal. Chem. 87, 216–229.

Deng, M., Xu, S.G., Chen, F.N., 2014. Enhanced chemiluminescence of the luminol-hydrogen peroxide system by BSA-stabilized Au nanoclusters as a peroxidase mimic and its application. Anal. Meth. 6, 3117–3123.

Hindson, C.M., Francis, P.S., Hanson, G.R., Adcock, J.L., Barnett, N.W., 2010. Mechanism of permanganate chemiluminescence. Anal. Chem. 82, 4174–4180.

Iranifam, M., 2014. Analytical applications of chemiluminescence methods for cancer detection and therapy. TRAC-Trend Anal. Chem 59, 156–183.

Jiang, J., Conroy, C.V., Kvetny, M.M., Lake, G.J., Padelford, J.W., Ahuja, T., Wang, G.L., 2014. Oxidation at the core-ligand interface of Au lipoicacid nanoclusters that enhances the near-IR luminescence. J. Phys. Chem. C 118, 20680–20687.

Liu, M.L., Lin, Z., Lin, J.M., 2010. A review on applications of chemiluminescence detection in food analysis. Anal. Chim. Acta 670, 1–10.

Luo, Z.T., Zheng, K.Y., Xie, J.P., 2014. Engineering ultrasmall water-soluble gold and silver nanoclusters for biomedical applications. Chem. Commun. 50, 5143–5155.

Ocana-Gonzalez, J.A., Ramos-Payan, M., Fernandez-Torres, R., Navarro, M.V., Bello-Lopez, M.A., 2014. Application of chemiluminescence in the analysis of wastewaters-a review. Talanta 122, 214–222.

Odio, O.F., Lartundo-Rojas, L., Santiago-Jacinto, P., Martinez, R., Reguera, E., 2014. Sorption of gold by the naked and thiol-capped magnetite nanoparticles: an XPs approach. J. Phys. Chem. C 118, 2776–2791.

Sun, J., Yang, F., Zhao, D., Yang, X.R., 2014. Highly sensitive real-time assay of inorganic pyrophosphatase activity based on the fluorescent gold nanoclusters. Anal. Chem. 86, 7883–7889.

Waseem, A., Yaqoob, M., Nabi, A., 2013. Analytical applications of flow injection chemiluminescence for the determination of pharmaceuticals-a review. Curr. Pharm. Anal. 9, 363–395.

Xie, J.P., Zheng, Y.G., Ying, J.Y., 2009. Protein-directed synthesis of highly fluorescent gold nanoclusters. J. Am. Chem. Soc. 131, 888–889.

Xiong, X.L., Tang, Y.L., Zhang, L.L., Zhao, S.L., 2015. A label-free fluorescent assay for free chlorine in drinking water based on protein-stabilized gold nanoclusters. Talanta 132, 790–795.

Xu, S.H., Lu, X., Yao, C.X., Huang, F., Jiang, H., Hua, W.H., Na, N., Liu, H.Y., Ouyang, J., 2014. A visual sensor array for pattern recognition analysis of proteins using novel blue-emitting fluorescent gold nanoclusters. Anal. Chem. 86, 11634–11639.

Yu, X., Wang, Q., 2011. The determination of copper ions based on sensitized chemiluminescence of silver nanoclusters. Microchim. Acta 173, 293–298.

Yu, X., Wang, Q., Liu, X., Luo, X., 2012. A sensitive chemiluminescence method for the determination of cysteine based on silver nanoclusters. Microchim. Acta 179, 323–328.

Yu, Y., New, S.Y., Xie, J.P., Su, X.D., Tan, Y.N., 2014. Protein-based florescent metal nanoclusters for small molecular drug screening. Chem. Commun. 50, 13805–13808.

Zhang, L.B., Wang, E.K., 2014. Metal nanoclusters: new fluorescent probes for sensors and bioimaging. Nano Today 9, 132–157.

Zhang, Z.F., Cui, H., Shi, M.J., 2006. Chemiluminescence accompanied by the reaction of gold nanoparticles with potassium permanganate. Phys. Chem. Chem. Phys. 8, 1017–1021.

Zhu, M.Z., Lanni, E., Garg, N., Bier, M.E., Jin, R.C., 2008. Kinetically controlled, high-yield synthesis of Au25 clusters. J. Am. Chem. Soc. 130, 1138–1139.

Please cite this article in press as: You, X., Li, Y. Direct chemiluminescence of fluorescent gold nanoclusters with classic oxidants for hydrogen peroxide sensing. Arabian Journal of Chemistry (2015), http://dx.doi.org/10.1016/j.arabjc.2015.05.019